

RESEARCH ARTICLE

Diffusion weighted imaging as a biomarker of retinoic acid induced myelomeningocele

Nathan Maassel^{1*}, James Farrelly¹, Daniel Coman², Mollie Freedman-Weiss¹, Samantha Ahle¹, Sarah Ullrich¹, Nicholas Yung¹, Fahmeed Hyder^{2,3}, David Stitelman⁴

1 Department of Surgery, Yale School of Medicine, New Haven, Connecticut, United States of America, **2** Department of Radiology and Biomedical Imaging, Yale School of Medicine, New Haven, Connecticut, United States of America, **3** Department of Biomedical Engineering, Yale School of Engineering & Applied Science, New Haven, Connecticut, United States of America, **4** Division of Pediatric Surgery, Department of Surgery, Yale School of Medicine, New Haven, Connecticut, United States of America

* nathan.maassel@yale.edu



Abstract

Neural tube defects are a common congenital anomaly involving incomplete closure of the spinal cord. Myelomeningocele (MMC) is a severe form in which there is complete exposure of neural tissue with a lack of skin, soft tissue, or bony covering to protect the spinal cord. The all-trans retinoic acid (ATRA) induced rat model of (MMC) is a reproducible, cost-effective means of studying this disease; however, there are limited modalities to objectively quantify disease severity, or potential benefits from experimental therapies. We sought to determine the feasibility of detecting differences between MMC and wild type (WT) rat fetuses using diffusion magnetic resonance imaging techniques (MRI). Rat dams were gavage-fed ATRA to produce MMC defects in fetuses, which were surgically delivered prior to term. Average diffusion coefficient (ADC) and fractional anisotropy (FA) maps were obtained for each fetus. Brain volumes and two anatomically defined brain length measurements (D1 and D2) were significantly decreased in MMC compared to WT. Mean ADC signal was significantly increased in MMC compared to WT, but no difference was found for FA signal. In summary, ADC and brain measurements were significantly different between WT and MMC rat fetuses. ADC could be a useful complementary imaging biomarker to current histopathologic analysis of MMC models, and potentially expedite therapeutic research for this disease.

OPEN ACCESS

Citation: Maassel N, Farrelly J, Coman D, Freedman-Weiss M, Ahle S, Ullrich S, et al. (2021) Diffusion weighted imaging as a biomarker of retinoic acid induced myelomeningocele. PLoS ONE 16(6): e0253583. <https://doi.org/10.1371/journal.pone.0253583>

Editor: Quan Jiang, Henry Ford Health System, UNITED STATES

Received: March 26, 2021

Accepted: June 8, 2021

Published: June 30, 2021

Copyright: © 2021 Maassel et al. This is an open access article distributed under the terms of the [Creative Commons Attribution License](https://creativecommons.org/licenses/by/4.0/), which permits unrestricted use, distribution, and reproduction in any medium, provided the original author and source are credited.

Data Availability Statement: All relevant data are within the manuscript and its [Supporting information](#) files.

Funding: The author(s) received no specific funding for this work.

Competing interests: The authors have declared that no competing interests exist.

Introduction

Spina bifida is a type of fetal malformation characterized by failure of neural tube closure during gestational development. The incidence of neural tube defects (NTD) is variable, but estimates range from 1–7 per 1000 live births and differ by region, ethnicity, and sex [1–3]. Myelomeningocele (MMC) is the most common and severe NTD, resulting in complete exposure of spinal cord and meninges at birth. The majority of MMC patients are also born with a Chiari II malformation, defined by downward displacement of their cerebellum and medulla, which can cause poor CSF outflow and hydrocephalus. The increased intracranial pressure

can lead to a host of other neurologic sequelae including cognitive dysfunction, dysphagia, and difficulty breathing in these patients, which often necessitates shunt placement [4, 5]. Exposure of the spinal cord to mechanical and chemical stressors during gestation leads to permanent neural injury characterized by urinary and fecal incontinence and complete paralysis of the lower extremities in most patients. MMC treatment options include pre- or post-natal surgery to correct the skin defect in addition to post-natal ventricular shunting. Neonatal mortality remains high for MMC babies at around 10%, and while many MMC patients go on to complete high school and attend college, only about 50% of survivors are capable of living independently as adults [6, 7].

Early *in utero* treatment for MMC remains an ongoing area of research, but, as there is no reliable objective way to analyze disease severity or treatment effectiveness in early gestation, an imaging biomarker that correlates with known histopathological findings would be critical. The all-trans retinoic acid (ATRA) induced MMC rat model is a reproducible and reliable model for testing novel therapies [8–10]. Although ATRA can produce MMC defects in a majority of exposed fetuses, it is difficult to determine structural and functional differences between prenatal and postnatal MMC and wild type (WT) pups. Magnetic Resonance Imaging (MRI) has been used to quantify the severity of Chiari malformations, and high-resolution computed tomography (CT) has been used to characterize vertebral body defects, but MRI and/or CT data has not been particularly useful in the quantitative comparison of defects themselves [11, 12]. This is important especially for experiments where defect coverage/correction *in utero* is the method of intervention. Currently, post-mortem histology is the primary way to demonstrate presumed potential benefit from prenatal therapies designed to cover the MMC defect prior to birth; however, histology requires euthanasia of the specimens and does not provide sufficient insight into structural or functional correlates. Ideally, an imaging biomarker test would objectively quantify neurologic injury in fetuses to more reliably monitor the results of a corrective intervention.

Diffusion Weighted Imaging (DWI) and Diffusion Tensor Imaging (DTI) are structural MRI techniques that quantify water diffusion in a specific region of tissue. These techniques have been previously used to evaluate spinal cord injury in various animal and human studies [13–18]. The apparent diffusion coefficient (ADC) is a DWI measurement that specifies the magnitude of water diffusion over a specific region, whereas fractional anisotropy (FA) is a DTI measurement that specifies the degree of directional diffusion of water [16]. Although ADC and FA are typically not mapped at histological resolution, they can provide cellular information since ADC can reflect degree of cellularity and FA can represent fiber directionality. We sought to investigate differences in ADC, FA and volumetric data of the central nervous system between WT and MMC groups as a proof of concept for potential future assessment in therapeutic studies.

Materials and methods

Retinoic acid induced MMC model

MMC rat fetuses were generated using previously described methodology [8–10, 19–23]. In short, time-dated pregnant Sprague-Dawley dams (Charles River Laboratories; Wilmington, MA) were gavage-fed 1cc of 40 mg/kg, 97% pure ATRA (Across Organics; Morris Plains, NJ) dissolved in olive oil (Whole Foods Market; Austin, TX) on day 10 of gestation. Dams underwent routine daily monitoring for hydration status, activity level, and maintenance of proper nutritional status. WT fetuses were generated using time-dated pregnant dams that did not undergo ATRA gavage. Two dams were used for MMC and two for WT. All animal use was in accordance with the guidelines of Yale University's Institutional Animal Care and Use

Committee. Approval was also granted from this same committee after review by the Yale Office of Animal Research Support (protocol #: 2017–11632).

MRI of brain and spinal cord

On gestational day 17, WT and MMC dams were euthanized via CO₂ followed by cervical dislocation. The fetuses (6 from MMC, 6 from WT) were then harvested and placed into a custom-built MRI-compatible tube filled with Fluorinert—an MRI susceptibility-matching fluid (Sigma-Aldrich). MRI images were obtained on an 11.7 T horizontal bore scanner (Bruker, Billerica, MA) with a bore size of 9 cm and maximum gradient strength of 400 mT/m, using a custom-made ¹H radio frequency volume coil (4 cm diameter). The DTI experiments were performed using a spin-echo diffusion-weighted sequence with 4 shots, a diffusion gradient of 6 ms and a delay between the two diffusion gradients of 12 ms. 16 contiguous slices of 0.5 mm thickness were acquired at a resolution of 180 × 110 with a field of view of 36mm × 22mm using a repetition time (TR) of 4s, an echo time (TE) of 21 ms and 12 averages. 20 different images were acquired for each slice, 15 corresponding to various non-collinear diffusion gradient directions with $b = 1,000 \text{ s mm}^{-2}$ and 5 with no diffusion gradients. The total acquisition time was 4.5 hours. Although data was acquired at high field (11.7T), no image correction was necessary. FA and ADC images were generated from the diffusion-weighted spin-echo images in BioImage Suite (<http://www.bioimagesuite.org/>).

The brain distances D1 and D2 were standardized using anatomic landmarks. D1 represents the distance from the lateral reticular nucleus to the frontal association cortex, while D2 represents the distance from the lateral reticular nucleus to the interpeduncular nucleus (Fig 1A and 1B, top). The brain volume was determined by manually drawing a region-of-interest (ROI) over the entire brain using the ADC map which provided the best image contrast, followed by calculation of the ROI volume (Fig 1A and 1B, bottom). The spinal cord was analyzed using a manually selected ROI over the lower spinal cord (Fig 2A and 2D), for which the average ADC and FA were calculated. Manual ROI determination was chosen due to inaccurate delineation when using an intensity-standardized threshold approach.

Statistical analysis

Averages and standard deviations were calculated for brain distances D1 and D2, brain volume, and spinal cord ADC and FA in BioImage Suite. Group comparisons were performed using a two-tailed Student's t-test in BioImage Suite. Statistical significance was considered $p < 0.05$.

Results

The brain size comparison between the MMC ($n = 6$) and WT ($n = 6$) groups used three separate measurements: brain volume and two distances D1 and D2, representing the distance from the lateral reticular nucleus to the frontal association cortex or the interpeduncular nucleus, respectively (Fig 1). Average distances D1 and D2 measured in WT specimens were significantly larger than MMC ($9.79 \pm 0.19 \text{ mm}$, D1 and $3.77 \pm 0.10 \text{ mm}$, D2 for WT vs $8.30 \pm 0.14 \text{ mm}$, D1 and $2.03 \pm 0.10 \text{ mm}$, D2 for MMC, $p < 0.0001$) (Fig 1 and Table 1). In addition, brain volume measurements for the WT group were significantly larger than those of the MMC group ($204 \pm 9 \text{ mm}^3$ for WT vs $173 \pm 7 \text{ mm}^3$ for MMC, $p < 0.0001$) (Fig 1 and Table 1).

The average ADC signal over the selected ROI in the spinal cord (Fig 2) was significantly higher in the MMC group when compared to the WT ($836 \pm 89 \mu\text{m}^2/\text{s}$ for MMC vs $566 \pm 37 \mu\text{m}^2/\text{s}$ for WT, $p < 0.0001$). There were no statistically significant differences ($p = 0.54$) in spinal cord FA between the two groups (Fig 2). The average volume of the selected ROI of the

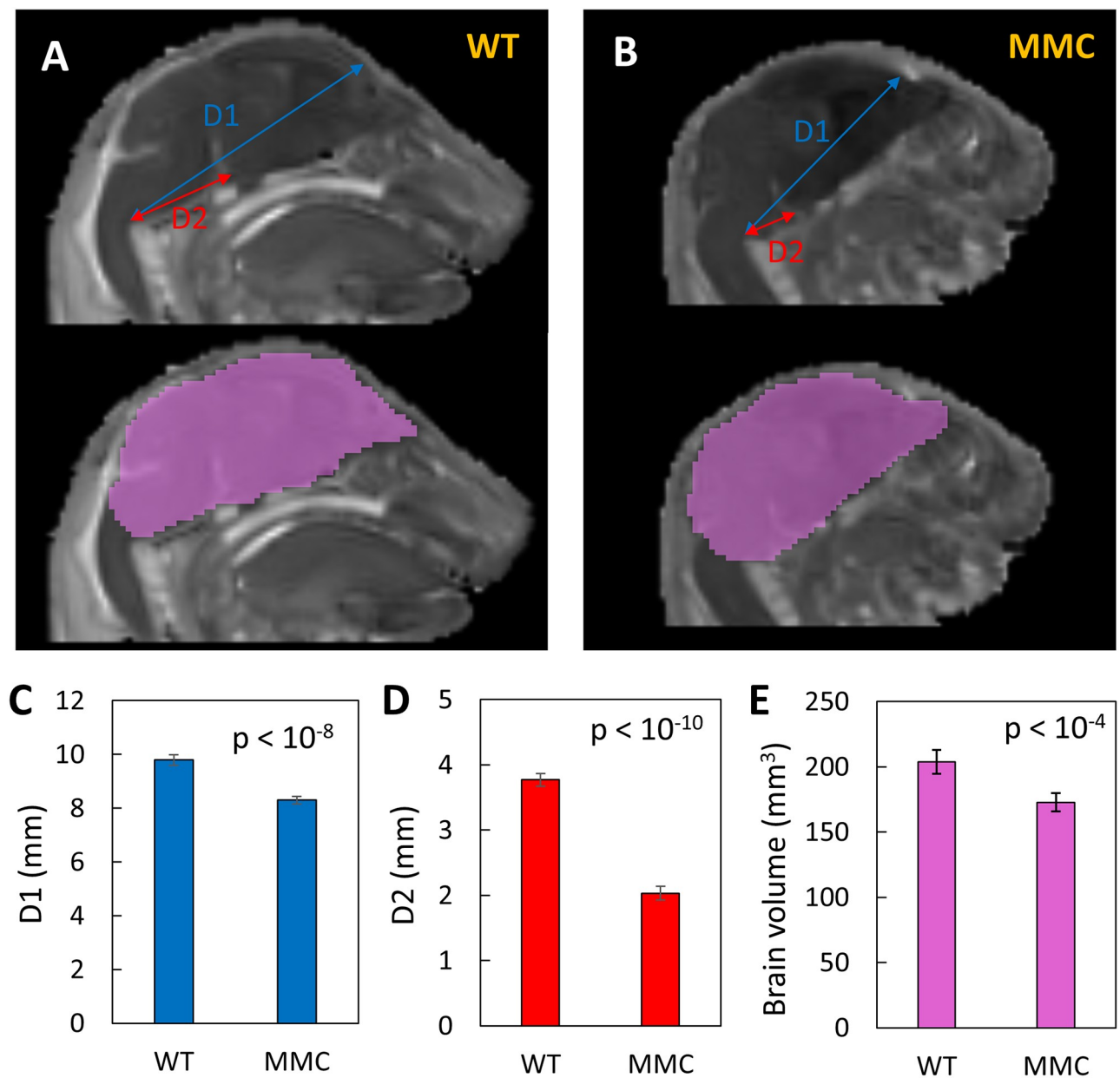


Fig 1. Measurements of brain size for the MMC and WT groups. Examples of D1 and D2 distances (top) and brain volume (bottom) in WT (A) and MMC (B) groups. D1 and D2 represent the distance from the lateral reticular nucleus to the frontal association cortex or the interpeduncular nucleus, respectively. The brain volume was determined by manually drawing a ROI over the entire brain using the ADC map which provided the best image contrast, followed by calculation of the ROI volume. The distances D1 (C) and D2 (D), and the brain volume (E) were significantly smaller in the MMC compared to the WT group.

<https://doi.org/10.1371/journal.pone.0253583.g001>

spinal cord used for ADC and FA analysis was $11.7 \pm 1.0 \text{ mm}^3$ for the WT group and $11.0 \pm 0.6 \text{ mm}^3$ for the MMC group (Table 1). The statistical comparison between WT and MMC demonstrates similar ROI volumes for both groups.

Discussion

This study investigated a novel method for comparing the structure of ATRA-induced MMC rat brains and spinal cords with those of WT rats. MMC fetuses were found to have smaller

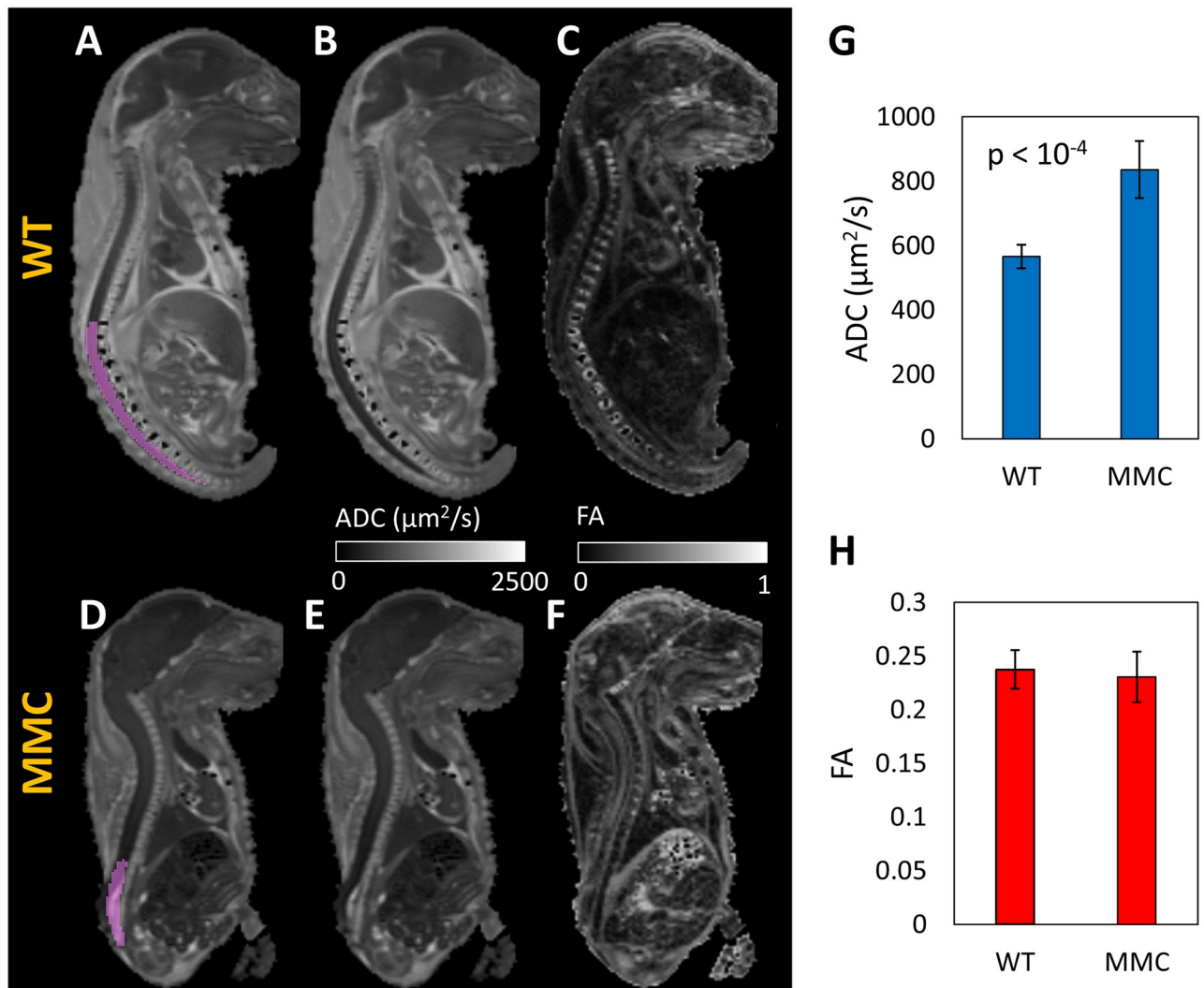


Fig 2. FA and ADC in the spinal cord measured over a selected lumbosacral ROI. Examples of selected spinal cord ROI (A, D), ADC maps (B, E) and FA maps (C, F), in WT and MMC fetuses. Statistically higher ADC ($p < 0.0001$) was measured in the MMC group (G). No significant differences were observed in the FA values when comparing the MMC and WT groups (H).

<https://doi.org/10.1371/journal.pone.0253583.g002>

brain length and volume in addition to higher ADC signal in the spinal cord compared to WT. There was no significant difference in the FA signal between the two groups. ADC signal and brain dimensions could be useful adjuncts for quantifying the effects of therapeutic interventions in the rat MMC model and may expedite clinical translation. The fact that ADC is higher

Table 1. Wild type vs myelomeningocele rat fetus brain, spine, FA, and ADC measurements.

	WT	std	MMC	std	p value
Brain Length D1, mm	9.79	0.19	8.3	0.14	<0.0001
Brain Length D2, mm	3.77	0.1	2.03	0.1	<0.0001
Brain Volume, mm ³	204	9	173	7	<0.0001
Spinal ROI Volume, mm ³	11.7	1	11	0.6	0.1100
FA	0.24	0.02	0.23	0.02	0.5400
ADC, μm ² /s	566	37	836	89	<0.0001

<https://doi.org/10.1371/journal.pone.0253583.t001>

in MMC with FA being indifferent from WT is significant. These data suggest that MMC spinal cords might have reduced cellularity but similar directionality of cellular connections when compared to WT specimens.

The ability to objectively quantify injury in animal models for MMC without causing harm to the fetus is essential to evaluating therapeutic strategies developed in the laboratory setting. Much of the current literature about in-utero treatment of MMC focuses on coverage or water-tight repair of the spina bifida defect prior to term and appropriately displays histological analyses to quantify success [21–27]. After development of a compelling novel MMC therapy, meaningful functional outcomes would provide a clear step towards human clinical translation; however, functional neurological evaluation is especially challenging in a sick small-animal model such as the ATRA-induced rat model. There are several composite scoring systems that exist for the assessment of neurologic function in rats, but these methods require survival to term, continuous monitoring, and are more commonly used in adult models for stroke and spinal cord injury [28, 29]. For this reason, utilization of non-invasive diffusion-based MRI to complement histologic evidence of defect coverage is extremely useful. Although future *in vivo* DWI studies are needed to establish this *ex vivo* DWI finding, it is anticipated that a 50% increase in ADC for MMC would be detectable even under the most modest MRI scanner situations.

The current understanding of the pathology of spinal cord injury in spina bifida involves a two-hit disease process, whereby a primary error in neural tube development is made significantly worse by secondary injury from chemical and mechanical damage to spinal cord tissue while *in utero* [30, 31]. In human applications of DTI, specific to spina bifida, there have been reports of abnormal white matter development and decreased FA signal, suggesting axonal injury [32]. Though our study found no significant difference in FA, the average ADC was significantly higher in the MMC rat fetuses compared to WT. One possible explanation for an increased ADC in the MMC fetuses is the increased water mobility due to extracellular edema and cell degeneration from the “second hit” in myelomeningocele pathogenesis. Although this is an ongoing area of research, there have been several studies detailing an increase in digestive enzymes within amniotic fluid of rats with MMC, as a possible mechanism for injury [33, 34]. In human spinal cord studies, ADC signal has been shown to increase with age related spinal cord degeneration, explained at least partially by chronic ischemia and natural degenerative changes [16]. This is in contrast to the decrease seen in ADC signal at 24 and 72 hours in acute rat spinal cord injury models [35]. Unlike the acute traumatic pathology of the rat spinal cord injury model, the pathologic timeline of MMC is likely more analogous to a chronic process; however, there is no baseline measurement of ADC or FA in the rat model of MMC for comparison. Apart from toxicity related to exposure in the amniotic environment, human studies of young patients with spina bifida suggest disruption of the sacral plexus as an additional pathophysiologic explanation for paralysis and genitourinary dysfunction in these patients. In a series of 10 patients age 8 to 16 years old, Haakma et al. demonstrated asymmetry and disorganization of the sacral plexus using DTI and fiber tractography [36]. These findings demonstrate the range of additional applications for diffusion MRI techniques that could be applied in the experimental and clinical setting to potentially measure MMC severity or improvement following a therapeutic intervention.

The limitations of this study are its relatively small group size ($n = 6$ in each group) and single gestational time point for analysis. Additionally, though the MRI data investigated in this study was obtained using a high field pre-clinical scanner (11.7T), we expect that the results would be reproducible at lower magnetic fields (i.e., 1.5T–7T). Water diffusion properties (like ADC and FA) are not field dependent, which makes MRI sequences such as DWI or DTI more translatable. Despite these limitations, the overarching purpose of this study was to pilot

structural and anatomical MRI techniques as possible methods for discerning MMC from WT as a step towards non-invasive monitoring of therapeutic success following a pre-natal intervention in the rat model of MMC. As experimental therapies for MMC move toward clinical trials, diffusion MRI may prove useful for post-therapy monitoring in humans as well, however these applications are beyond the scope of this study. Future directions for this line of research include a therapeutic group and a wider range of gestational ages to term (E21).

Conclusions

Analysis of objective neurologic outcomes in the rat model of MMC is challenging during the early stages of pup development. ADC and brain size measurements using diffusion MRI could provide a non-invasive platform to quantify both severity of injury and objective treatment response in the ATRA-induced rat MMC model. Future studies that analyze the long-term functional neurological outcomes of treated and untreated MMC pups will be crucial for determining the validity of non-invasive, prenatal MRI for measuring prenatal MMC therapy response.

Supporting information

S1 Dataset. Individual animal data with summary statistics and corresponding figures. (XLSX)

Author Contributions

Conceptualization: James Farrelly, Daniel Coman, Fahmeed Hyder, David Stitelman.

Data curation: Nathan Maassel, James Farrelly, Daniel Coman, Mollie Freedman-Weiss, Samantha Ahle, Sarah Ullrich, Nicholas Yung, David Stitelman.

Formal analysis: Daniel Coman, Mollie Freedman-Weiss, Samantha Ahle, Sarah Ullrich.

Investigation: Nathan Maassel, James Farrelly, Mollie Freedman-Weiss, Samantha Ahle, Sarah Ullrich, Nicholas Yung.

Methodology: Nathan Maassel, Daniel Coman, Fahmeed Hyder.

Project administration: Fahmeed Hyder.

Supervision: Fahmeed Hyder, David Stitelman.

Writing – original draft: Nathan Maassel, David Stitelman.

Writing – review & editing: Nathan Maassel, James Farrelly, Daniel Coman, Mollie Freedman-Weiss, Samantha Ahle, Sarah Ullrich, Nicholas Yung, Fahmeed Hyder, David Stitelman.

References

1. Khoshnood B, Loane M, de Walle H, Arriola L, Addor MC, Barisic I, et al. Long term trends in prevalence of neural tube defects in Europe: population based study. *BMJ*. 2015; 351:h5949. Epub 2015/11/26. <https://doi.org/10.1136/bmj.h5949> PMID: 26601850.
2. Frey L, Hauser WA. Epidemiology of neural tube defects. *Epilepsia*. 2003; 44 Suppl 3:4–13. Epub 2003/06/07. <https://doi.org/10.1046/j.1528-1157.44.s3.2.x> PMID: 12790881.
3. Blencowe H, Kanacherla V, Moorthie S, Darlison MW, Modell B. Estimates of global and regional prevalence of neural tube defects for 2015: a systematic analysis. *Ann N Y Acad Sci*. 2018; 1414(1):31–46. Epub 2018/01/25. <https://doi.org/10.1111/nyas.13548> PMID: 29363759.

4. Naidich TP, McLone DG, Fulling KH. The Chiari II malformation: Part IV. The hindbrain deformity. *Neuroradiology*. 1983; 25(4):179–97. Epub 1983/01/01. <https://doi.org/10.1007/BF00540232> PMID: 6605491.
5. Elgamal EA. Natural history of hydrocephalus in children with spinal open neural tube defect. *Surg Neurol Int*. 2012; 3:112. Epub 2012/10/23. <https://doi.org/10.4103/2152-7806.101801> PMID: 23087828.
6. Tennant PW, Pearce MS, Bythell M, Rankin J. 20-year survival of children born with congenital anomalies: a population-based study. *Lancet*. 2010; 375(9715):649–56. Epub 2010/01/23. [https://doi.org/10.1016/S0140-6736\(09\)61922-X](https://doi.org/10.1016/S0140-6736(09)61922-X) PMID: 20092884.
7. Bowman RM, McLone DG, Grant JA, Tomita T, Ito JA. Spina bifida outcome: a 25-year prospective. *Pediatr Neurosurg*. 2001; 34(3):114–20. Epub 2001/05/19. <https://doi.org/10.1159/000056005> PMID: 11359098.
8. Danzer E, Schwarz U, Wehrli S, Radu A, Adzick NS, Flake AW. Retinoic acid induced myelomeningocele in fetal rats: characterization by histopathological analysis and magnetic resonance imaging. *Exp Neurol*. 2005; 194(2):467–75. Epub 2005/05/17. <https://doi.org/10.1016/j.expneurol.2005.03.011> PMID: 15893307.
9. Danzer E, Kiddoo DA, Redden RA, Robinson L, Radu A, Zderic SA, et al. Structural and functional characterization of bladder smooth muscle in fetal rats with retinoic acid-induced myelomeningocele. *Am J Physiol Renal Physiol*. 2007; 292(1):F197–206. Epub 2006/08/31. <https://doi.org/10.1152/ajprenal.00001.2006> PMID: 16940565.
10. Danzer E, Radu A, Robinson LE, Volpe MV, Adzick NS, Flake AW. Morphologic analysis of the neuromuscular development of the anorectal unit in fetal rats with retinoic acid induced myelomeningocele. *Neurosci Lett*. 2008; 430(2):157–62. Epub 2007/12/08. <https://doi.org/10.1016/j.neulet.2007.10.048> PMID: 18063303.
11. Dionigi B, Brazzo JA 3rd, Ahmed A, Feng C, Wu Y, Zurakowski D, et al. Trans-amniotic stem cell therapy (TRASCET) minimizes Chiari-II malformation in experimental spina bifida. *J Pediatr Surg*. 2015; 50(6):1037–41. Epub 2015/05/02. <https://doi.org/10.1016/j.jpedsurg.2015.03.034> PMID: 25929798.
12. Barbe MF, Adiga R, Gordiienko O, Pleshko N, Selzer ME, Krynska B. Micro-computed tomography assessment of vertebral column defects in retinoic acid-induced rat model of myelomeningocele. *Birth Defects Res A Clin Mol Teratol*. 2014; 100(6):453–62. Epub 2014/06/24. <https://doi.org/10.1002/bdra.23254> PMID: 24954432.
13. Vedantam A, Jirjis MB, Schmit BD, Wang MC, Ulmer JL, Kurpad SN. Diffusion tensor imaging of the spinal cord: insights from animal and human studies. *Neurosurgery*. 2014; 74(1):1–8; discussion; quiz <https://doi.org/10.1227/NEU.0000000000000171> PMID: 24064483.
14. Werner H, Lopes J, Tonni G, Araujo E Junior. Physical model from 3D ultrasound and magnetic resonance imaging scan data reconstruction of lumbosacral myelomeningocele in a fetus with Chiari II malformation. *Childs Nerv Syst*. 2015; 31(4):511–3. Epub 2015/02/18. <https://doi.org/10.1007/s00381-015-2641-6> PMID: 25686895.
15. DeBoy CA, Zhang J, Dike S, Shats I, Jones M, Reich DS, et al. High resolution diffusion tensor imaging of axonal damage in focal inflammatory and demyelinating lesions in rat spinal cord. *Brain*. 2007; 130(Pt 8):2199–210. <https://doi.org/10.1093/brain/awm122> PMID: 17557778.
16. Mamata H, Jolesz FA, Maier SE. Apparent diffusion coefficient and fractional anisotropy in spinal cord: age and cervical spondylosis-related changes. *J Magn Reson Imaging*. 2005; 22(1):38–43. <https://doi.org/10.1002/jmri.20357> PMID: 15971186.
17. Liu C, Yang D, Li J, Li D, Yang M, Sun W, et al. Dynamic diffusion tensor imaging of spinal cord contusion: A canine model. *J Neurosci Res*. 2018; 96(6):1093–103. <https://doi.org/10.1002/jnr.24222> PMID: 29485189.
18. Kelley BJ, Harel NY, Kim CY, Papademetris X, Coman D, Wang X, et al. Diffusion tensor imaging as a predictor of locomotor function after experimental spinal cord injury and recovery. *J Neurotrauma*. 2014; 31(15):1362–73. <https://doi.org/10.1089/neu.2013.3238> PMID: 24779685.
19. Danzer E, Zhang L, Radu A, Bebbington MW, Liechty KW, Adzick NS, et al. Amniotic fluid levels of glial fibrillary acidic protein in fetal rats with retinoic acid induced myelomeningocele: a potential marker for spinal cord injury. *Am J Obstet Gynecol*. 2011; 204(2):178 e1–11. Epub 2011/02/03. <https://doi.org/10.1016/j.ajog.2010.09.032> PMID: 21284970.
20. Mackenzie TC, Flake AW. Human mesenchymal stem cells persist, demonstrate site-specific multipotential differentiation, and are present in sites of wound healing and tissue regeneration after transplantation into fetal sheep. *Blood Cells Mol Dis*. 2001; 27(3):601–4. Epub 2001/08/03. <https://doi.org/10.1006/bcmd.2001.0424> PMID: 11482873.
21. Watanabe M, Li H, Roybal J, Santore M, Radu A, Jo J, et al. A tissue engineering approach for prenatal closure of myelomeningocele: comparison of gelatin sponge and microsphere scaffolds and bioactive

- protein coatings. *Tissue Eng Part A*. 2011; 17(7–8):1099–110. Epub 2010/12/07. <https://doi.org/10.1089/ten.TEA.2010.0390> PMID: 21128864.
22. Watanabe M, Jo J, Radu A, Kaneko M, Tabata Y, Flake AW. A tissue engineering approach for prenatal closure of myelomeningocele with gelatin sponges incorporating basic fibroblast growth factor. *Tissue Eng Part A*. 2010; 16(5):1645–55. Epub 2009/12/04. <https://doi.org/10.1089/ten.TEA.2009.0532> PMID: 19954327.
 23. Watanabe M, Kim AG, Flake AW. Tissue engineering strategies for fetal myelomeningocele repair in animal models. *Fetal Diagn Ther*. 2015; 37(3):197–205. Epub 2014/07/26. <https://doi.org/10.1159/000362931> PMID: 25060746.
 24. Farrelly JS, Bianchi AH, Ricciardi AS, Buzzelli GL, Ahle SL, Freedman-Weiss MR, et al. Alginate micro-particles loaded with basic fibroblast growth factor induce tissue coverage in a rat model of myelomeningocele. *J Pediatr Surg*. 2019; 54(1):80–5. Epub 2018/11/12. <https://doi.org/10.1016/j.jpedsurg.2018.10.031> PMID: 30414695.
 25. Shieh HF, Tracy SA, Hong CR, Chalphin AV, Ahmed A, Rohrer L, et al. Transamniotic stem cell therapy (TRASCET) in a rabbit model of spina bifida. *J Pediatr Surg*. 2019; 54(2):293–6. <https://doi.org/10.1016/j.jpedsurg.2018.10.086> PMID: 30518492.
 26. Mann LK, Won JH, Trenton NJ, Garnett J, Snowise S, Fletcher SA, et al. Cryopreserved human umbilical cord versus acellular dermal matrix patches for in utero fetal spina bifida repair in a pregnant rat model. *J Neurosurg Spine*. 2019; 32(2):321–31. <https://doi.org/10.3171/2019.7.SPINE19468> PMID: 31675701.
 27. Watanabe M, Li H, Kim AG, Weilerstein A, Radu A, Davey M, et al. Complete tissue coverage achieved by scaffold-based tissue engineering in the fetal sheep model of Myelomeningocele. *Biomaterials*. 2016; 76:133–43. <https://doi.org/10.1016/j.biomaterials.2015.10.051> PMID: 26520044.
 28. Ahmed RU, Alam M, Zheng YP. Experimental spinal cord injury and behavioral tests in laboratory rats. *Heliyon*. 2019; 5(3):e01324. Epub 2019/03/25. <https://doi.org/10.1016/j.heliyon.2019.e01324> PMID: 30906898.
 29. Schaar KL, Brenneman MM, Savitz SI. Functional assessments in the rodent stroke model. *Exp Transl Stroke Med*. 2010; 2(1):13. Epub 2010/07/21. <https://doi.org/10.1186/2040-7378-2-13> PMID: 20642841.
 30. Drewek MJ, Bruner JP, Whetsell WO, Tulipan N. Quantitative analysis of the toxicity of human amniotic fluid to cultured rat spinal cord. *Pediatr Neurosurg*. 1997; 27(4):190–3. <https://doi.org/10.1159/000121250> PMID: 9577972.
 31. Adzick NS. Fetal myelomeningocele: natural history, pathophysiology, and in-utero intervention. *Semin Fetal Neonatal Med*. 2010; 15(1):9–14. <https://doi.org/10.1016/j.siny.2009.05.002> PMID: 19540177.
 32. Hasan KM, Eluvathingal TJ, Kramer LA, Ewing-Cobbs L, Dennis M, Fletcher JM. White matter micro-structural abnormalities in children with spina bifida myelomeningocele and hydrocephalus: a diffusion tensor tractography study of the association pathways. *J Magn Reson Imaging*. 2008; 27(4):700–9. <https://doi.org/10.1002/jmri.21297> PMID: 18302204.
 33. Talabani H, Dreux S, Luton D, Simon-Bouy B, Le Fiblec B, Col JY, et al. Fetal anal incontinence evaluated by amniotic fluid digestive enzyme assay in myelomeningocele spina bifida. *Pediatric research*. 2005; 58(4):766–70. <https://doi.org/10.1203/01.PDR.0000180539.40399.93> PMID: 16189207.
 34. Agarwal R, Thornton ME, Fonteh AN, Harrington MG, Chmait RH, Grubbs BH. Amniotic fluid levels of phospholipase A2 in fetal rats with retinoic acid induced myelomeningocele: the potential "second hit" in neurologic damage. *J Matern Fetal Neonatal Med*. 2016; 29(18):3003–8. <https://doi.org/10.3109/14767058.2015.1112373> PMID: 26513600.
 35. Li XH, Li JB, He XJ, Wang F, Huang SL, Bai ZL. Timing of diffusion tensor imaging in the acute spinal cord injury of rats. *Sci Rep*. 2015; 5:12639. <https://doi.org/10.1038/srep12639> PMID: 26220756.
 36. Haakma W, Dik P, ten Haken B, Froeling M, Nieuvelstein RA, Cuppen I, et al. Diffusion tensor magnetic resonance imaging and fiber tractography of the sacral plexus in children with spina bifida. *J Urol*. 2014; 192(3):927–33. <https://doi.org/10.1016/j.juro.2014.02.2581> PMID: 24769033.